

Update on gravitational wave signals from post-inflationary phase transitions

H. Kolesova^a and M. Laine^b

^a*Faculty of Science and Technology, University of Stavanger,
4036 Stavanger, Norway*

^b*AEC, Institute for Theoretical Physics, University of Bern,
Sidlerstrasse 5, CH-3012 Bern, Switzerland*

Abstract

In view of recent interest in high-frequency detectors, broad features of gravitational wave signals from phase transitions taking place soon after inflation are summarized. The influence of the matter domination era that follows the slow-roll stage is quantified in terms of two equilibration rates. Turning to the highest-frequency part of the spectrum, we show how it is constrained by the fact that the bubble distance scale must exceed the mean free path.

1. Introduction

A cosmological first-order phase transition may produce a gravitational wave signal [1–3]. The signal is expected to be peaked, with the peak frequency proportional to the phase transition temperature, T_* . In particular, phase transitions at the QCD scale, $T_* \sim 100$ MeV, could yield a signal for the high end of the pulsar timing array observation window ($f_0 \sim 10^{-8} \dots 10^{-6}$ Hz); those at the weak scale, with $T_* \sim 100$ GeV, would match the LISA frequency range ($f_0 \sim 10^{-4} \dots 10^{-1}$ Hz); whereas exotic phase transitions with $T_* \sim 1 \dots 100$ TeV could leave an imprint to be discovered by DECIGO ($f_0 \sim 10^{-1} \dots 10^1$ Hz) or the Einstein Telescope ($f_0 \sim 10^1 \dots 10^3$ Hz) [4]. Phase transitions at much higher scales, related perhaps to GUTs, might in turn be probed at the GHz...THz range that has become of recent interest [5].

The signal from high-scale phase transitions has been estimated in ref. [5]. The purpose of the current study, which was influenced by recent model investigations [6, 7], is to derive an upper bound for a phase-transition-induced gravitational wave energy density in the GHz...THz range. We establish its peak frequency, and elaborate on the effect of a matter domination era that follows slow-roll inflation (cf., e.g., refs. [8–10]), if the relevant equilibration rates are small compared with the Hubble rate. The main differences with respect to ref. [5] will be recapitulated in the conclusions (cf. sec. 5). Before that, we review the main features of the background evolution in the reheating epoch (cf. sec. 2), broad features of the gravitational wave signal originating from phase transitions (cf. sec. 3), and the maximal strain that this physics can lead to (cf. sec. 4).

2. Background evolution

We have in mind a usual single-field inflationary scenario. As the slow-roll stage ends, the inflaton starts oscillating and the temperature reaches a maximal value. There is normally a period in which inflaton oscillations dominate the overall energy density, before the energy density of a thermal plasma takes over.

We assume the matter content during this time to reside in three components:

- **inflaton**, φ , with energy density e_φ .
- **“dark sector”**, defined as the one undergoing a phase transition. The low-temperature phase of the dark sector is assumed massive (i.e. non-relativistic), due to confinement or Higgs mechanism, so it does not exert pressure. Its energy density is denoted by e_d .
- **“visible sector”**, constituted of Standard Model like particles, which are effectively massless during the epoch under consideration. Its energy density is denoted by e_v .

Adding sectors together, we denote $e_{ij} \equiv e_i + e_j$, notably $e_{\text{dv}} \equiv e_{\text{d}} + e_{\text{v}}$. The overall energy density is then $e \equiv e_{\varphi\text{dv}}$, with the corresponding Hubble rate given by

$$H^2 = \frac{8\pi e}{3m_{\text{pl}}^2}, \quad m_{\text{pl}} = 1.22091 \times 10^{19} \text{ GeV}. \quad (2.1)$$

In general we parametrize moments in the reheating epoch by the value of H . Motivated by Planck data [11], we also conservatively set $H \leq H_{\text{max}} \equiv 10^{-5} m_{\text{pl}}$.

We model the dynamics of this coupled system by equations of the type

$$\dot{e}_i + 3H(e_i + p_i) \simeq -\sum_j \Gamma_{ij}(e_j - e_{j,\text{eq}}). \quad (2.2)$$

Summing over i , the Friedmann equation needs to be recovered, implying $\sum_i \Gamma_{ij} = 0$. The equilibrium values, $e_{j,\text{eq}}$, represent the fixed point that would be attained if the system had infinite time. In order to simplify the setup, we assume that the visible sector is effectively thermalized, $e_{\text{v}} \approx e_{\text{v,eq}}$. Only two rates are assumed to have a large influence:¹

- **inflaton interaction rate**, $\Upsilon \equiv \Gamma_{\varphi\varphi} = -\Gamma_{\text{d}\varphi}$. In general Υ would be a function of the dark sector temperature, but we assume that the part originating from vacuum decays dominates. A possible temperature dependence can subsequently be mimicked by interpolating between various constant values.
- **dark sector interaction rate**, $\Gamma \equiv \Gamma_{\text{dd}} = -\Gamma_{\text{vd}}$.

Assuming also an initial state with $e_{\varphi} \gg e_{\varphi,\text{eq}}$ and $e_{\text{d}} \gg e_{\text{d,eq}}$, we are then faced with

$$\dot{e}_{\varphi} + 3H(e_{\varphi} + p_{\varphi}) \simeq -\Upsilon e_{\varphi}, \quad (2.3)$$

$$\dot{e}_{\text{d}} + 3H(e_{\text{d}} + p_{\text{d}}) \simeq +\Upsilon e_{\varphi} - \Gamma e_{\text{d}}, \quad (2.4)$$

$$\dot{e}_{\text{v}} + 3H(e_{\text{v}} + p_{\text{v}}) \simeq +\Gamma e_{\text{d}}. \quad (2.5)$$

We define

$$H_+ \equiv \max\{\Upsilon, \Gamma\}, \quad H_- \equiv \min\{\Upsilon, \Gamma\}, \quad (2.6)$$

with the corresponding scale factors denoted by a_+ and a_- , respectively. We now consider the solution of eqs. (2.3)–(2.5) in various regimes, making use of the labelling in fig. 1.

Domain (1). During the reheating period, the inflaton is oscillating faster than the Hubble rate, satisfying then $\ddot{\varphi} - \partial_{\varphi}V \simeq 0$. After multiplication with $\dot{\varphi}$, this can be integrated into $\frac{1}{2}\dot{\varphi}^2 - V \simeq 0$, implying that $p_{\varphi} \simeq 0$, $e_{\varphi} \simeq \dot{\varphi}^2$. The regime in which these equations apply corresponds to a matter domination era. Recalling $e_{\varphi} \gg \max\{e_{\text{d}}, e_{\text{v}}\}$, so that $H^2 = 8\pi e_{\varphi}/(3m_{\text{pl}}^2)$, and $\Upsilon \ll H$, whereby the right-hand side can be omitted, eq. (2.3) yields

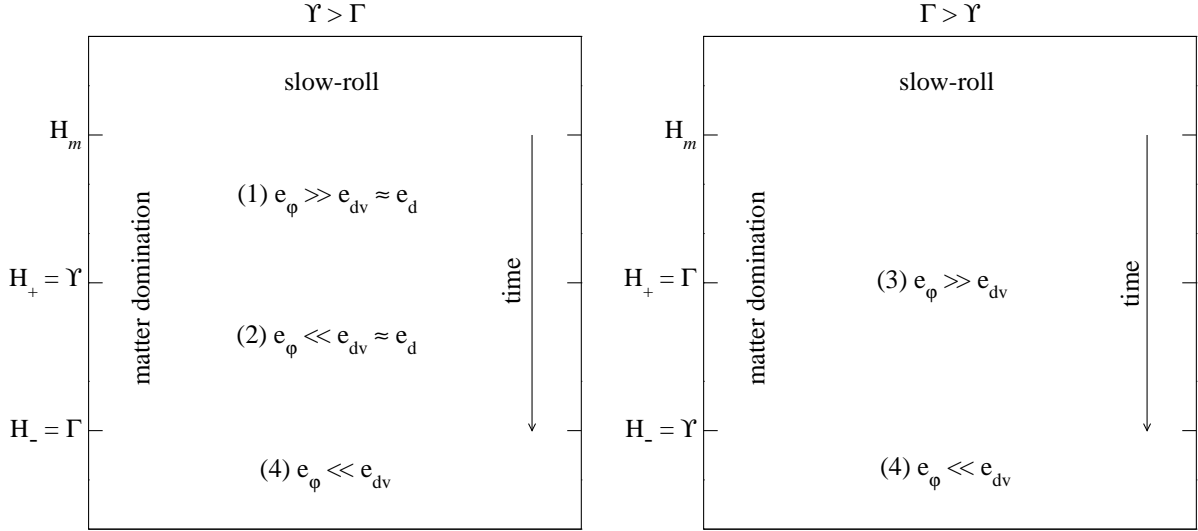


Figure 1: Cartoons of the key epochs of the reheating period. Here H_m denotes the moment at which the slow-roll expansion ends and the oscillation (i.e. matter domination) period begins, and Υ and Γ two rates that characterize the dynamics (cf. eqs. (2.3)–(2.5)).

$8\pi e_\varphi/(3m_{\text{pl}}^2) \simeq [2/(3t)]^2$. This in turn implies $H/H_m \simeq t_m/t$, $(e_\varphi/e_{\varphi,m}) \simeq (t_m/t)^2$, $a/a_m \simeq (t/t_m)^{2/3}$, and $H_m t_m \simeq 2/3$, where t_m denotes the time at which matter domination starts.

The key for us is the solution of eq. (2.4) in the presence of e_φ . With the given assumptions, the right-hand side of eq. (2.4) simplifies to $+\Upsilon e_\varphi$. Replacing t through H as an integration variable, the evolution equation can be re-expressed as

$$-\partial_H e_d + \frac{2(1+w_d)}{H} e_d \simeq \frac{\Upsilon m_{\text{pl}}^2}{4\pi}, \quad w_d \equiv \frac{p_d}{e_d}. \quad (2.7)$$

The general solution is

$$\boxed{H \gg \Upsilon \gg \Gamma}: \quad e_\varphi a^3 \simeq \text{const}, \quad e_d \simeq C H^{2(1+w_d)} + \frac{m_{\text{pl}}^2 \Upsilon H}{4\pi(1+2w_d)}, \quad (2.8)$$

where C is an integration constant. If $w_d > -\frac{1}{2}$, the latter term dominates at late times.

An important consequence of eq. (2.8) is that we can determine the phase transition moment, denoted by H_* . If $e_{d,*}$ is the dark energy density at the phase transition, and omitting the subdominant term from the right-hand side, eq. (2.8) can be inverted into

$$H_* \gg \Upsilon \gg \Gamma: \quad H_* \simeq 4\pi(1+2w_*) \frac{e_{d,*}}{m_{\text{pl}}^2 \Upsilon}. \quad (2.9)$$

¹In this setup the dark sector serves as a mediator between the inflaton and the visible sector, however we hope that the results model qualitatively also situations in which more than two rate coefficients play a role.

Domain (2). Because of $\Upsilon \gg H$, φ has equilibrated in this domain, and plays little role. Given that $\Gamma \ll H$, the right-hand side of eq. (2.4) can be omitted, and we are faced with

$$\dot{e}_d + 3H(e_d + p_d) \simeq 0. \quad (2.10)$$

Thus we obtain

$$\boxed{\Upsilon \gg H \gg \Gamma} : \quad e_\varphi \simeq e_{\varphi, \text{eq}}, \quad e_d a^{3(1+w_d)} \simeq \text{const}. \quad (2.11)$$

Domain (3). In this domain we can sum together eqs. (2.4) and (2.5), finding

$$\dot{e}_{\text{dv}} + 3H(e_{\text{dv}} + p_{\text{dv}}) \simeq +\Upsilon e_\varphi. \quad (2.12)$$

The solution is like for eq. (2.7), yielding a variant of eq. (2.8),

$$\boxed{\begin{array}{l} H \gg \Gamma \gg \Upsilon \\ \Gamma \gg H \gg \Upsilon \end{array}} : \quad e_\varphi a^3 \simeq \text{const}, \quad e_{\text{dv}} \simeq \frac{m_{\text{pl}}^2 \Upsilon H}{4\pi(1+2w_{\text{dv}})}, \quad w_{\text{dv}} \equiv \frac{p_{\text{dv}}}{e_{\text{dv}}}. \quad (2.13)$$

Domain (4). In this domain the solution is like in eq. (2.11), except that the dark and visible sectors have equilibrated,

$$\boxed{\min\{\Upsilon, \Gamma\} \gg H} : \quad e_\varphi \simeq e_{\varphi, \text{eq}}, \quad e_{\text{dv}} a^{3(1+w_{\text{dv}})} \stackrel{w_{\text{dv}} \simeq \frac{1}{3}}{\simeq} e_{\text{dv}} a^4 \simeq \text{const}. \quad (2.14)$$

If the phase transition takes place in this domain, then its gravitational wave signature is not affected by matter domination, and it redshifts as usual [4, 12].

3. Broad characteristics of the gravitational wave signal

Considering a phase transition taking place in one of the domains mentioned above, we wish to work out its gravitational wave signature. Here we are concerned with an upper bound, omitting the complicated hydrodynamics by which it gets formed (cf., e.g., ref. [4]). The assumption is that immediately after the transition, gravitational waves carry the energy density $e_{\text{gw},*}$. The first task is to estimate which energy fraction this corresponds to today.

We focus on gravitational waves whose wavelength was within the horizon at the time of their formation.² Their energy density scales with expansion like radiation. The relation to the critical energy density today, when the scale factor is a_0 , is

$$\Omega_{\text{gw},0} \equiv \frac{e_{\text{gw},0}}{e_{\text{crit}}} = \frac{e_{\text{gw},*} a_*^4}{e_{\text{crit}} a_0^4} = \underbrace{\frac{e_{\text{gw},*}}{e_{\varphi,*}}}_{\text{first}} \underbrace{\frac{e_{\varphi,*} a_*^4}{e_- a_-^4}}_{\text{second}} \underbrace{\frac{e_- a_-^4}{e_{\text{crit}} a_0^4}}_{\text{third}}, \quad (3.1)$$

²The study of phase transitions leading to longer wavelengths has also been initiated [13], however as will be seen in sec. 4 (cf. fig. 3), such cases do not extend to the frequencies that are of most interest to us.

where e_{crit} is the current critical energy density and the notation e_{\pm} , a_{\pm} corresponds to that introduced around eq. (2.6). We have expressed the result as a product of three factors, which can be estimated as follows, considering the domains in fig. 1.

Domain (1). For the *first* factor in eq. (3.1), we parametrize the energy density released into gravitational radiation by its relation to the dark sector energy density at that time. Making use of eq. (2.9), this then yields

$$\frac{e_{\text{gw},*}}{e_{\varphi,*}} = \frac{e_{\text{gw},*} e_{\text{d},*}}{e_{\text{d},*} e_{\varphi,*}} \stackrel{(2.9)}{\simeq} \frac{e_{\text{gw},*}}{e_{\text{d},*}} \frac{m_{\text{pl}}^2 \Upsilon H_*}{4\pi(1+2w_*)e_{\varphi,*}} \simeq \frac{e_{\text{gw},*}}{e_{\text{d},*}} \frac{2\Upsilon}{3(1+2w_*)H_*}. \quad (3.2)$$

For the *second* factor in eq. (3.1), we obtain

$$\frac{e_{\varphi,*} a_*^4}{e_- a_-^4} \simeq \frac{e_{\varphi,*} a_*^4 e_+ a_+^4}{e_+ a_+^4 e_- a_-^4} \simeq \left(\frac{e_{\varphi,+}}{e_{\varphi,*}}\right)^{1/3} \left(\frac{e_{\text{d},-}}{e_{\text{d},+}}\right)^{1/3} e_{\text{d},+} \simeq e_{\varphi,+} \left(\frac{e_{\text{d},-}}{e_{\varphi,*}}\right)^{1/3} \simeq \left(\frac{H_-}{H_*}\right)^{2/3}. \quad (3.3)$$

For the *third* factor, we express a via $s_{\text{dv}} a_{\text{dv}}^3 \simeq \text{constant}$, resulting in

$$\frac{e_- a_0^4}{e_{\text{crit}} a_0^4} \simeq \frac{e_- T_0^4}{e_{\text{crit}} T_-^4} \left(\frac{s_0/T_0^3}{s_-/T_-^3}\right)^{4/3} = \frac{e_{\gamma,0}}{e_{\text{crit}}} \frac{e_-/T_-^4}{e_{\gamma,0}/T_0^4} \left(\frac{g_{s,0}}{g_{s,-}}\right)^{4/3} = \underbrace{\frac{g_{s,0}^{4/3} e_{\gamma,0}}{g_{\gamma,0} e_{\text{crit}} 10^{2/3}} \frac{1}{g_{s,-}} \frac{g_{e,-}}{g_{s,-}} \left(\frac{100}{g_{s,-}}\right)^{1/3}}_{\approx 1.65 \times 10^{-5}/h^2}, \quad (3.4)$$

where we parametrized the thermal energy and entropy densities as $e_{\text{dv}} = g_e \pi^2 T^4/30$, $s_{\text{dv}} = g_s 2\pi^2 T^3/45$. For the numerical value, we have employed $e_{\gamma,0}/e_{\text{crit}} = 2.473 \times 10^{-5}/h^2$, where h is the reduced Hubble rate, as well as $g_{s,0} \simeq 3.92$, which is related to though not studied as much as the parameter N_{eff} that captures the energy density of the universe after neutrino decoupling (cf. ref. [14, sec. 3.1] for a discussion). Multiplying together eqs. (3.2)–(3.4), finally yields

$$h^2 \Omega_{\text{gw},0} \stackrel{\text{domains (1),(3)}}{\simeq} 1.65 \times 10^{-5} \frac{g_{e,-}}{g_{s,-}} \left(\frac{100}{g_{s,-}}\right)^{1/3} \left(\frac{\Upsilon}{H_*}\right) \left(\frac{H_-}{H_*}\right)^{2/3} \frac{2}{3(1+2w_*)} \frac{e_{\text{gw},*}}{e_{\text{dv},*}}. \quad (3.5)$$

In the last step we have replaced $e_{\text{d},*} \rightarrow e_{\text{dv},*}$ in domain (1), using the fact that $e_{\text{v},*} \ll e_{\text{d},*}$ there, because then the result is also valid in domain (3).

Domain (2). In this domain, we replace $e_{\varphi,*} \rightarrow e_{\text{d},*}$ in eq. (3.1), because $e_{\varphi} \approx e_{\varphi,\text{eq}} \ll e_{\text{d}}$. For the *second* factor after this modification, we still find the same result as in eq. (3.3),

$$\frac{e_{\text{d},*} a_*^4}{e_- a_-^4} \simeq \left(\frac{e_{\text{d},-}}{e_{\text{d},*}}\right)^{1/3} \simeq \left(\frac{H_-}{H_*}\right)^{2/3}. \quad (3.6)$$

The final result becomes

$$h^2 \Omega_{\text{gw},0} \stackrel{\text{domain (2)}}{\simeq} 1.65 \times 10^{-5} \frac{g_{e,-}}{g_{s,-}} \left(\frac{100}{g_{s,-}}\right)^{1/3} \left(\frac{H_-}{H_*}\right)^{2/3} \frac{e_{\text{gw},*}}{e_{\text{dv},*}}. \quad (3.7)$$

Eq. (3.5) goes over into (3.7) at the moment $H_* = 2\Upsilon/[3(1+2w_*)] \simeq \Upsilon$.

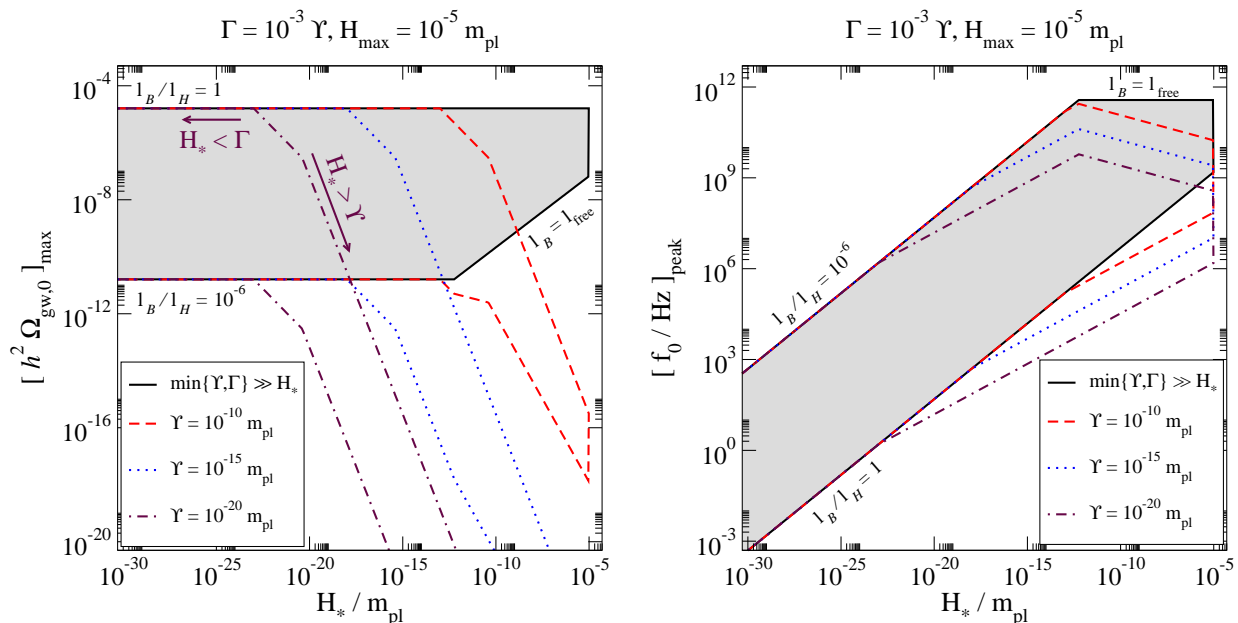


Figure 2: Left: the maximal gravitational energy fraction, from eqs. (3.5), (3.7) and (3.8), obtained with $e_{\text{gw},*}/e_{\text{dv},*} \rightarrow (\ell_B/\ell_H)\theta(\ell_B - \ell_{\text{free}})$, where $\ell_B/\ell_H \in (10^{-6}, 1)$. We have here chosen $\Gamma = 10^{-3}\Upsilon$ for illustration. Only large equilibration rates, $\min\{\Upsilon, \Gamma\} \gg H_*$, permit for a sizable effect, otherwise the signal gets diluted. Right: the peak frequency, from eqs. (3.12) and (3.13).

Domain (3). Though intermediate steps differ, we recover eq. (3.5).

Domain (4). If the transition takes place in the usual thermal epoch, then eq. (3.3) is to be omitted, with the result originating from eq. (3.4) evaluated at the transition point,

$$h^2 \Omega_{\text{gw},0}^{\text{domain (4)}} \simeq 1.65 \times 10^{-5} \frac{g_{e,*}}{g_{s,*}} \left(\frac{100}{g_{s,*}} \right)^{1/3} \frac{e_{\text{gw},*}}{e_{\text{dv},*}}. \quad (3.8)$$

Role of mean free path. If microscopic information about the hydrodynamics is inserted, we can be more precise about the factor $e_{\text{gw},*}/e_{\text{dv},*}$ in eqs. (3.5), (3.7) and (3.8). In particular, since gravitational waves are tensor excitations, their production rate is proportional to a bubble length scale breaking translational invariance, which we denote in the following by ℓ_B . In fact, a quadrupole moment requires a quadratic dependence on ℓ_B , but this could be partly compensated for by a long duration of a process (cf., e.g., ref. [15]). Furthermore, if ℓ_B goes towards zero, the production rate does not vanish, but is then taken over by that from thermal fluctuations [16]. In the so-called hydrodynamic regime, the fluctuation rate is proportional to the shear viscosity, which in turn is proportional to the mean free path, ℓ_{free} . We treat the fluctuation contribution as a separate source (cf. sec. 4). To get a conservative

upper bound for the phase transition contribution, we set $e_{\text{gw},*}/e_{\text{dv},*} \rightarrow (\ell_B/\ell_H)\theta(\ell_B - \ell_{\text{free}})$, where $\ell_H \equiv H_*^{-1}$ is the Hubble radius. The value of ℓ_B/ℓ_H is strongly model dependent, so we vary it in the range $1 \dots 10^{-6}$, indicating the variation as an error band.

We still need to estimate the numerical value of ℓ_{free} . If $\alpha \lesssim 1$ is a characteristic coupling, then the mean free path is $\sim 1/(\alpha^2 T)$, however we would not like to make assumptions about the magnitude of the coupling. Therefore we set

$$\ell_{\text{free}} \simeq \frac{1}{\pi T_*}. \quad (3.9)$$

The most conservative estimate is obtained when ℓ_{free} is smallest, or T_* is highest. This is the case when the dark sector energy density saturates H_* , i.e. when $\Upsilon > H_*$. The results obtained after determining ℓ_{free} with this recipe are shown in fig. 2(left).³

Peak frequency. The ratio ℓ_B/ℓ_H plays an important role also for the peak frequency of the gravitational wave spectrum. As we push towards high temperatures, with correspondingly small values of ℓ_H , we must make sure that we do not underestimate ℓ_B , i.e. we must maintain $\ell_B > \ell_{\text{free}}$. The peak gravitational wave frequency today, f_0 , is expressed as

$$f_{0,\text{peak}} \equiv \frac{a_*}{a_0} \frac{\theta(\ell_B - \ell_{\text{free}})}{\ell_B} = \underbrace{\frac{a_*}{a_-}}_{\text{first}} \underbrace{\frac{a_- H_*}{a_0}}_{\text{second}} \frac{\ell_H \theta(\ell_B - \ell_{\text{free}})}{\ell_B}. \quad (3.10)$$

Starting with domain (1) in fig. 1, the *first* factor can be approximated as in eq. (3.3), yielding $(H_-/H_*)^{2/3}$, whereas the *second* factor can be expressed like in radiation domination,

$$\begin{aligned} \frac{a_- H_*}{a_0} &= T_0 \frac{a_-}{a_0} \frac{H_*}{T_0} = T_0 \left(\frac{s_0/T_0^3}{s_-/T_-^3} \right)^{1/3} \frac{H_*}{T_-} = T_0 \left(\frac{g_{s,0}}{g_{s,-}} \right)^{1/3} \left(\frac{\pi^2 g_{e,-}}{30} \frac{8\pi}{3m_{\text{pl}}^2} \frac{1}{H_-^2} \right)^{1/4} H_* \\ &\simeq \underbrace{\frac{g_{s,0}^{1/3}}{10^{1/6}} \left(\frac{4\pi^3}{45} \right)^{1/4}}_{\approx 1.38} T_0 \left(\frac{g_{e,-}}{g_{s,-}} \right)^{1/4} \left(\frac{100}{g_{s,-}} \right)^{1/12} \left(\frac{H_*}{H_-} \right)^{1/2} \left(\frac{H_*}{m_{\text{pl}}} \right)^{1/2}, \end{aligned} \quad (3.11)$$

where $T_0 = 3.57 \times 10^{11}$ Hz. Putting the factors together yields

$$f_{0,\text{peak}} \stackrel{\text{domains (1),(2),(3)}}{\simeq} 1.38 T_0 \left(\frac{g_{e,-}}{g_{s,-}} \right)^{1/4} \left(\frac{100}{g_{s,-}} \right)^{1/12} \left(\frac{H_-}{H_*} \right)^{1/6} \left(\frac{H_*}{m_{\text{pl}}} \right)^{1/2} \frac{\ell_H \theta(\ell_B - \ell_{\text{free}})}{\ell_B}. \quad (3.12)$$

As indicated, the same formula is obtained in domains (2) and (3). The standard formula for a radiation-dominated epoch is recovered by omitting the *first* factor in eq. (3.10), and

³We have set $g_e \simeq g_s \simeq 106.75$, $w \simeq 1/3$, but these choices have no qualitative effect.

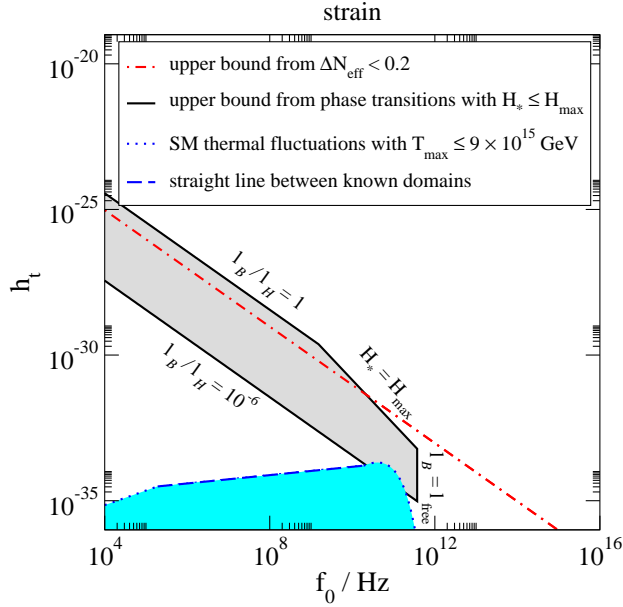


Figure 3: A combination of the two panels in fig. 2 with $\min\{\Upsilon, \Gamma\} \gg H_*$, expressed in terms of the strain h_t from eq. (4.1), compared with the ΔN_{eff} bound from eq. (4.4), as well as the thermal fluctuation result with $T_{\text{max}} \leq 9 \times 10^{15} \text{ GeV}$, corresponding to $H_{\text{max}} \leq 10^{-5} m_{\text{pl}}$. The last part consists of two known domains, namely an IR tail from hydrodynamic fluctuations at small f_0 [16] and a peak part from elementary particle scatterings at large f_0 [17]; we have connected these with a straight line. The amplitude of the peak part increases in BSM scenarios (cf. refs. [18, 19] for concrete examples).

by replacing the point between the matter and radiation dominated epochs by the phase transition point, whereby

$$f_{0,\text{peak}} \stackrel{\text{domain (4)}}{\simeq} 1.38 T_0 \left(\frac{g_{e,*}}{g_{s,*}} \right)^{1/4} \left(\frac{100}{g_{s,*}} \right)^{1/12} \left(\frac{H_*}{m_{\text{pl}}} \right)^{1/2} \frac{\ell_H \theta(\ell_B - \ell_{\text{free}})}{\ell_B}. \quad (3.13)$$

The results of eqs. (3.12) and (3.13) are plotted in fig. 2(right).

4. Maximal gravitational strain from post-inflationary phase transitions

We have seen in sec. 3 that a phase transition during a matter-dominated epoch, present if $\min\{\Upsilon, \Gamma\} < H_*$, leads to a suppressed gravitational wave signal (cf. eqs. (3.5) and (3.7)), and reduces the peak frequency of a given transition (cf. eq. (3.12)).⁴ In the present section we wish to find the maximal possible signal, at the highest possible peak frequency, and therefore consider the regime $\min\{\Upsilon, \Gamma\} > H_*$. In this case the transition takes place during radiation

⁴It can be verified that there is suppression also in the gravitational strain, to be introduced below.

domination. We represent the results in the same form as in fig. 2 of ref. [5], underlining then also the differences with respect to this standard reference.

For quantifying the gravitational wave signal, it has become standard to employ the experimentally meaningful strain, rather than the theoretically preferred energy density. However, there are a number of possibilities for its definition. In terms of eq. (3.1), the current gravitational energy density can be expressed as $e_{\text{gw},0} = m_{\text{pl}}^2 \sum_{i,j} \langle \dot{h}_{ij}^t \dot{h}_{ij}^t \rangle / (32\pi)$, where h_{ij}^t is a metric perturbation in the tensor channel, and $\langle \dots \rangle$ can be interpreted as a time average. The critical energy density is defined as $e_{\text{crit}} \equiv 3m_{\text{pl}}^2 H_0^2 / (8\pi)$, where H_0 is the current Hubble rate. We go to frequency space ($\partial_t \rightarrow \omega_0 = 2\pi f_0$), and replace the sum over polarizations by a numerical factor (4, for two polarization states and an additional factor for the symmetry in $i \leftrightarrow j$), whereby $h_{ij}^t \rightarrow h_t$. In the absence of spectral information, we may effectively assign all the energy density to the peak frequency, $f_{0,\text{peak}}$. Then the strain can be defined as

$$\Omega_{\text{gw},0} \equiv \frac{4\pi^2 f_{0,\text{peak}}^2 h_t^2(f_{0,\text{peak}})}{3H_0^2}, \quad H_0 = h \times 3.241 \times 10^{-18} \text{ Hz}. \quad (4.1)$$

Alternatively, if spectral information is available, we can parametrize a differential spectrum,

$$\frac{d\Omega_{\text{gw},0}}{d \ln f_0} \equiv \frac{4\pi^2 f_0^2 h_{t(\text{alt})}^2(f_0)}{3H_0^2}. \quad (4.2)$$

Writing

$$\frac{d\Omega_{\text{gw},0}}{d \ln f_0} = s(f_0) \frac{d\Omega_{\text{gw},0}}{d \ln f_0} \Big|_{f_0=f_{0,\text{peak}}}, \quad s(f_{0,\text{peak}}) \equiv 1, \quad (4.3)$$

we see that $h_t^2(f_{0,\text{peak}}) = h_{t(\text{alt})}^2(f_{0,\text{peak}}) \int_{-\infty}^{\infty} d \ln f_0 s(f_0)$. Thus the definitions agree at $f_{0,\text{peak}}$ if $\int_{-\infty}^{\infty} d \ln f_0 s(f_0) \simeq 1.0$.⁵ Adopting eq. (4.1), the results of fig. 2 are replotted in fig. 3.

We compare the phase transition result with two other considerations. The first is the parameter N_{eff} , characterizing the energy density carried by additional relativistic species at the time of primordial nucleosynthesis. If we write the gravitational energy density at that time as $e_{\text{gw},\text{bbn}} \equiv \Delta N_{\text{eff}} (7/8)(4/11)^{4/3} e_{\gamma,\text{bbn}}$, and redshift until today, then

$$\begin{aligned} \Omega_{\text{gw},0} &= \frac{e_{\text{gw},\text{bbn}} a_{\text{bbn}}^4}{e_{\text{crit}} a_0^4} = \Delta N_{\text{eff}} \left(\frac{s_0/T_0^3}{s_{\text{bbn}}/T_{\text{bbn}}^3} \right)^{4/3} \frac{7}{8} \left(\frac{4}{11} \right)^{4/3} \left(\frac{e_{\gamma,\text{bbn}}/T_{\text{bbn}}^4}{e_{\gamma,0}/T_0^4} \right) \frac{e_{\gamma,0}}{e_{\text{crit}}} \\ &= \underbrace{\Delta N_{\text{eff}} \left(\frac{g_{s,0}}{g_{s,\text{bbn}}} \right)^{4/3} \frac{7}{8} \left(\frac{4}{11} \right)^{4/3} \left(\frac{g_{\gamma,\text{bbn}}}{g_{\gamma,0}} \right) \frac{e_{\gamma,0}}{e_{\text{crit}}}}_{\approx 5.62 \times 10^{-6} / h^2}. \end{aligned} \quad (4.4)$$

We then interpret the upper bound $\Delta N_{\text{eff}} \leq 0.2$ [20] as a bound on $h_t^2(f_{0,\text{peak}})$ like in eq. (4.1).

⁵This assumption can be justified up to $\mathcal{O}(1)$ for some templates of phase transition spectra.

The second comparison concerns the irreducible background that originates from thermal fluctuations. This contribution is strongly dependent on the maximal temperature reached in the early universe. Evaluating the result by setting T to the temperature corresponding to H_{\max} , $T_{\max} \simeq 9 \times 10^{15} \text{ GeV}$, the dotted curve in fig. 3 is obtained, this time as an actual spectrum in accordance with eq. (4.2).⁶ Like for phase transitions (cf. fig. 2), a period of matter domination, present if $\min\{\Upsilon, \Gamma\} \ll H_{\max}$, would reduce the signal.

5. Conclusions

Our main findings can be summarized as follows. For phase transitions taking place soon after inflation, the gravitational wave signal is suppressed by a matter domination epoch, in an analytically quantifiable manner (cf. eqs. (3.5) and (3.7)), unless all equilibration rates are larger than the Hubble rate at the time of the transition. In the latter case (which could be realized for instance in models leading to a “strong regime” of warm inflation, or if the phase transition takes place after matter domination has ended), the phase transition signal can in principle saturate the N_{eff} bound, at $f_0 < 20 \text{ GHz}$ (cf. fig. 3). However, whether this actually happens depends on model-dependent characteristics of the phase transition. At $f_0 > 100 \text{ GHz}$, in contrast, the phase transition signal must merge with the irreducible background from thermal fluctuations (cf. fig. 3). The reason is that at distances less than the mean free path, “bubbles” are nothing but regular thermal fluctuations. We note that the latter physics seems to be missing from the considerations leading to fig. 2 of ref. [5].⁷

Acknowledgements

We thank Simona Procacci for helpful discussions. The work of H.K. was supported by the Research Council of Norway under the FRIPRO Young Research Talent grant no. 335388.

References

- [1] E. Witten, *Cosmic separation of phases*, Phys. Rev. D 30 (1984) 272.
- [2] C.J. Hogan, *Gravitational radiation from cosmological phase transitions*, Mon. Not. Roy. Astron. Soc. 218 (1986) 629.
- [3] M. Kamionkowski, A. Kosowsky and M.S. Turner, *Gravitational radiation from first-order phase transitions*, Phys. Rev. D 49 (1994) 2837 [astro-ph/9310044].

⁶The peak part comes from ref. [17], which considered physical momenta around $k \sim \pi T$. The spectrum is also known in the hydrodynamic domain $k \ll T$ [16], or even $k \ll H$ [21]. In between these domains, no computation exists to date, and our interpolation is simply a straight line.

⁷In addition, the IR tail from hydrodynamic fluctuations appears to have been underestimated there.

- [4] C. Grojean and G. Servant, *Gravitational waves from phase transitions at the electroweak scale and beyond*, Phys. Rev. D 75 (2007) 043507 [hep-ph/0607107].
- [5] N. Aggarwal *et al*, *Challenges and opportunities of gravitational-wave searches at MHz to GHz frequencies*, Living Rev. Rel. 24 (2021) 4 [2011.12414].
- [6] H. Kolesova, M. Laine and S. Procacci, *Maximal temperature of strongly-coupled dark sectors*, JHEP 05 (2023) 239 [2303.17973].
- [7] M.A. Buen-Abad, J.H. Chang and A. Hook, *Gravitational wave signatures from reheating*, Phys. Rev. D 108 (2023) 036006 [2305.09712].
- [8] D.J.H. Chung, E.W. Kolb and A. Riotto, *Production of massive particles during reheating*, Phys. Rev. D 60 (1999) 063504 [hep-ph/9809453].
- [9] J. Ellis, M. Lewicki and V. Vaskonen, *Updated predictions for gravitational waves produced in a strongly supercooled phase transition*, JCAP 11 (2020) 020 [2007.15586].
- [10] F. Ertas, F. Kahlhoefer and C. Tasillo, *Turn up the volume: listening to phase transitions in hot dark sectors*, JCAP 02 (2022) 014 [2109.06208].
- [11] Y. Akrami *et al* [Planck Collaboration], *Planck 2018 results. X. Constraints on inflation*, Astron. Astrophys. 641 (2020) A10 [1807.06211].
- [12] P. Schwaller, *Gravitational Waves from a Dark Phase Transition*, Phys. Rev. Lett. 115 (2015) 181101 [1504.07263].
- [13] L. Giombi and M. Hindmarsh, *General relativistic bubble growth in cosmological phase transitions*, 2307.12080.
- [14] K. Saikawa and S. Shirai, *Primordial gravitational waves, precisely: the role of thermodynamics in the Standard Model*, JCAP 05 (2018) 035 [1803.01038].
- [15] M. Hindmarsh, S.J. Huber, K. Rummukainen and D.J. Weir, *Gravitational Waves from the Sound of a First Order Phase Transition*, Phys. Rev. Lett. 112 (2014) 041301 [1304.2433].
- [16] J. Ghiglieri and M. Laine, *Gravitational wave background from Standard Model physics: qualitative features*, JCAP 07 (2015) 022 [1504.02569].
- [17] J. Ghiglieri, G. Jackson, M. Laine and Y. Zhu, *Gravitational wave background from Standard Model physics: Complete leading order*, JHEP 07 (2020) 092 [2004.11392].
- [18] A. Ringwald, J. Schütte-Engel and C. Tamarit, *Gravitational waves as a big bang thermometer*, JCAP 03 (2021) 054 [2011.04731].
- [19] P. Klose, M. Laine and S. Procacci, *Gravitational wave background from non-Abelian reheating after axion-like inflation*, JCAP 05 (2022) 021 [2201.02317].
- [20] N. Aghanim *et al* [Planck Collaboration], *Planck 2018 results. VI. Cosmological parameters*, Astron. Astrophys. 641 (2020) A6; *ibid.* 652 (2021) C4 (E) [1807.06209].
- [21] P. Klose, M. Laine and S. Procacci, *Gravitational wave background from vacuum and thermal fluctuations during axion-like inflation*, JCAP 12 (2022) 020 [2210.11710].